Laser and Particle Beams (2014), *32*, 487–493.

doi:10.1017/S0263034614000421

A novel numerical calculation method for electron guns

Y.F. KANG,[1] J. ZHAO,[1] J.Y. ZHAO,[1,2] AND T.T. TANG[1]

[1]Key Laboratory for Physical Electronics and Devices of the Ministry of Education, Xi'an Jiaotong University, Xi'an, People's Republic of China
[2]School of Science, Chang'an University, Xi'an, People's Republic of China

(Received 10 March 2014; Accepted 18 June 2014)

Abstract

The problem of initial thermal velocity and the space charge effect of electron guns in numerical simulations have been investigated deeply. In general, the current software can meet the engineering requirements. However, the electron's initial thermal velocity and the space charge effect lack sufficient consideration. The above two factors significantly limit the performances of electron guns. Moreover, the parameters of electron guns are approximated based on a limited number of electron trajectories. Thus, the statistical distribution of the beam electron resulting from its initial thermal velocity is not considered adequately in present software. This paper introduces the equivalent meridional projected trajectory equation and the curvilinear axis evolution theory of the current density of toroidal electron sub-beam, and subsequently the current and charge density distributions in electron guns can be derived through iteration calculation. Based upon, the virtual crossover of an electron gun is determined by its current density distribution. As well as, a relevant numerical algorithm is developed and the related program is modified based on the popular commercial software SOURCE. Tungsten cathode guns, LaB6 cathode guns, field mission guns and Pierce guns are simulated respectively by examples. The calculations prove that the modified software is effective and practical.

Keywords: Electron gun; Space charge; Initial thermal velocity; Numerical simulation

1. INTRODUCTION

Electron guns are fundamental components of electron optical equipments and instruments. However, their performance significantly limits the entire electron optics system (Ozur *et al*., 2003). Due to the complexity of structures and physical processes, the design and analysis of electron guns requires calculation by numerical methods. At present, the professional software available such as EGUN, TWTCAD, and ORION, etc., can neither give satisfactory computation precision nor have wide applicability. Rather than the above ones, the software SOURCE can give more precise results for almost all types of electron guns. However, certain factors detailed below have not been considered carefully in SOURCE, hence affecting the computation precision in some cases.

(1) The longitudinal thermal velocity effects: With Child's law describing the emission current density calculation of thermal cathodes (Zhu & Munro, 1989), the effects of longitudinal thermal velocity is not taken into account in SOURCE.

(2) The transverse thermal velocity effects and the calculation of electron rays: Cult theorem (Culter & Hines, 1955) is introduced in SOURCE. However, it is difficult to treat the electron thermal velocity effects by Cult theorem because the physical discussion of Cult theorem relies on simple linear assumptions. To calculate space charge density distributions, three-dimensionional (3D) electron rays must be achieved whether using the laminar flow method or the ray-tracing method previously (Hawkes & Kasper, 1989). However, the 3D computation is defective in principle for rotational symmetric electron guns. Moreover, the treatment of the 3D rays is very complicated.

(3) The calculation method of the electron guns parameter: The determination of the virtual crossover of electron guns is based on the finite electron rays in SOURCE. In fact, the statistical distribution of electron beams caused by the initial thermal velocity effect cannot adequately be taken into account using this method.

To solve the above problems, SOURCE is modified using the following methods. (1) Introducing the curved-axis electron optical theory in a meridional plane. This theory based

Address correspondence and reprint requests to: Y. F. Kang, Key Laboratory for Physical Electronics and Devices of the Ministry of Education, Xi'an Jiaotong University, Xi'an, 710049, People's Republic of China. E-mail: yfkang@mail.xjtu.edu.cn

on the following assumptions (Tang & Kang, 2005), (a) The guns are rotationally symmetric; (b) The beam is divided into many toroidal sub-beam units. Moreover, each sub-beam is so small that the initial current density at the cathode can be considered uniform within each unit; (c) The acceleration voltage is not very high so that the relativistic effect can be ignored. According to the above assumptions, the curved-axis electron optical theory in a meridional plane for calculating the evolution of the current density distribution of toroidal sub-beams is proposed. The concepts of equivalent acceleration potential and projection trajectories in meridional plane are introduced. Projection central trajectories based on these concepts were calculated and used as curvilinear optical axes for neighboring electrons with different initial thermal velocities. The curvilinear axis paraxial ray equation and the second-order aberrations are derived in local orthogonal coordinates. From this theory, the evolution equation of the current density distribution of the sub-beam units is derived; hence the total current and charge density distributions in the guns can be obtained giving a better treatment of the space charge effect and the initial thermal velocity effect. This method is very compact and practical for calculating round electron guns. Moreover, the initial thermal velocity effect and the space charge effect are handled better and more easily; in particular, the electron trajectories are non-planar curves with torsion because of magnetic fields. With this method introduced into SOURCE, this software is easy to program compared with other previously published methods (Burdovitsin & Oka, 2008; Septier, 1983; Villa & Luccio, 1997; Weber, 1967). (2) Determining the virtual intersection of electron guns by the current density distribution. After using the above method to compute the current density distribution of the sub-beam units, at the exit plane of electron guns, the distance to the axis and the slope of the central rays and current density at the axis direction for each sub-beam unit can be derived. Then, we assume that the potential is equivalent near the electron gun region. Using the above curved-axis electron optical theory, the virtual current density distribution of the gun region can be derived. The position with the maximum axial current density is the position of the virtual intersection.

2. THE CURVED-AXIS THEORY OF THE CURRENT DENSITY DISTRIBUTION EVOLUTION OF TOROIDAL SUB-BEAMS

In non-relativistic approximation, the electron projection trajectory equations in rotationally symmetrical electrical and magnetic fields in cylindrical coordinates (z, r, ψ) are as follows (Hawkes & Kasper, 1989; Stratton, 1941; Tang, 1986):

$$\begin{cases} r'' = \dfrac{1+r'^2}{2Q}\left(\dfrac{\partial Q}{\partial r} - r'\dfrac{\partial Q}{\partial z}\right) \\ Q = U* + \dfrac{e}{2m_0}\left(\dfrac{rA+C}{r}\right)^2, \end{cases} \tag{1}$$

where Q is called the equivalent meridional potential (the r coordinate varies with z). It includes not only the electric and magnetic fields, but also the initial angular momentum term C. U_* denotes the accelerating potential. These projection trajectory equations are very convenient for analysis and design of electron guns. As an ordinary differential equation, Eq. (1) is equivalent to the following variational equation (Tang, 1996):

$$\delta \int \sqrt{Q(r,z)}ds = 0. \tag{2}$$

Obviously, due to equivalent meridional potential Q and meridional plane projection trajectory of rotationally symmetrical systems introduced, the electron motion in three-dimensional (3D) space can be projected onto a two-dimensional (2D) plane. For the numerical simulations of the electron guns, the electron beam emitted from the cathode is divided into many toroidal sub-beam units.

A projection central trajectory is selected in each sub-beam as the curved optical axis of other adjacent electrons. These central trajectories are planar without torsion. Therefore, local orthogonal coordinates (x, z) are adopted where the axes are along the tangent (z) and normal (x) directions. There is a lateral statistical distribution of the electron current density in a sub-beam resulting from the thermal movement of the beam electrons. This distribution depends on the applied electric and magnetic fields as well as the space-charge field. Its evolution is dependent on the motion of all of the electrons within the sub-beam unit. Electron trajectories near to the curvilinear axis are derived using the curvilinear optical theory. As the ray equation is nonlinear, an approximation is made. At first, near to the curved axis, the equivalent meridional potential Q is expanded as a Taylor series in x:

$$Q = Q_0(z) + Q_1(z)x + Q_2(z)x^2 + Q_3(z)x^3 + \cdots, \tag{3}$$

where $Q_0(z)$ denotes the meridional potential along the curved axis, and the coefficients satisfy:

$$Q_1(z) = \frac{\partial Q}{\partial x}|_{x=0},\ Q_2(z) = \frac{1}{2}\frac{\partial^2 Q}{\partial x^2}|_{x=0},\ \cdots$$

In local orthogonal coordinates, the variation of Eq. (2) takes the following form (Tang, 1982):

$$\delta \int \mu dz = \delta \int Q dz = \delta \int \sqrt{Q}\sqrt{x'^2 + (1+kx)^2}dz = 0, \tag{4}$$

where μ is the integrand function of the variational equation, and k denotes the curvature of the optical axis, related to Q by:

$$\mathrm{k} = -\frac{Q_1}{2Q_0}. \tag{5}$$

https://doi.org/10.1017/S0263034614000421 Published online by Cambridge University Press

This ensures that the curved optical axis is a real trajectory. Introducing Eq. (3) into Eq. (4), expending μ as a series according to the powers of x and x' to the second order, we obtain:

$$\begin{aligned}\mu = \mu_0 + \mu_1 + \mu_2 = \sqrt{Q_0} + \sqrt{Q_0}(k + \frac{Q_1}{2Q_0})x \\ + \sqrt{Q_0}(\frac{Q_2}{Q_0} + \frac{kQ_1}{2Q_0} - \frac{Q_1^2}{4Q_0^2})x^2 + \sqrt{Q_0}x'^2\end{aligned}. \tag{6}$$

By introducing Eq. (6) into Eq. (4), the Euler equation for the variational equation is obtained:

$$\frac{d}{dz}[\frac{\partial}{\partial x'}(\mu_0 + \mu_1 + \mu_2)] = \frac{\partial}{\partial x}(\mu_0 + \mu_1 + \mu_2). \tag{7}$$

Substituting Eqs. (5) and (6) into Eq. (7), we obtain the following curved-axis paraxial trajectory equation:

$$\frac{d^2x}{dz^2} + \frac{Q_0'}{2Q_0}\frac{dx}{dz} + \left(\frac{Q_1^2}{2Q_0^2} - \frac{Q_2}{Q_0}\right)x = 0. \tag{8}$$

This homogeneous equation is called the paraxial trajectory equation. Its solution x_g can be formed by two linearly independent special solutions $g(z)$ and $h(z)$. The initial conditions of $g(z)$ and $h(z)$ are:

$$\begin{cases} g(z_0) = 1,\ g'(z_0) = 0 \\ h(z_0) = 0,\ h'(z_0) = 1 \end{cases}. \tag{9}$$

Hence the solution of the paraxial trajectory equation for initial coordinate x_0 and slope x_0' can be expressed as:

$$\begin{cases} x_g(z) = x_0 g(z) + x_0' h(z) \\ x_g'(z) = x_0 g'(z) + x_0' h'(z) \end{cases}. \tag{10}$$

The current density distribution of a sub-beam at the initial plane is a function of x_0 and x_0'. For thermal emission cathodes, the transverse mean energy of the thermal electrons is KT, where T is the cathode temperature and K denotes the Boltzmann constant. The directional distribution of the current density at the emitting point is a cosine function:

$$dj = \frac{j_0}{\pi}\cos\gamma d\Omega, \tag{11}$$

where j denotes the current density, and γ is of the angle relative to the local normal to the initial surface. It is assumed that j_0 denotes the current density at the initial emitting plane. After acceleration, there is an increase at a given plane in the electron energy $e(u\text{-}u_0)$ in the longitudinal direction, and the angular distribution becomes (Morrell *et al.*, 1974; Munro, 1997):

$$dj = \frac{e(u-u_0)}{KT} j_0 \cos\gamma \times \exp(-\frac{e(u-u_0)}{KT}\sin^2\gamma) d\Omega, \tag{12}$$

It is assumed that the initial current density of the toroidal sub-beam unit is uniform at the initial plane. Considering Eq. (12), the initial distribution can be defined as:

$$f(z_0, x_0, x_0') = N rect(\frac{x_0}{2b})\exp(-\frac{x_0'^2}{\alpha^2}), \tag{13}$$

where $2b$ is the width of the initial annular unit and N is a constant.

$$\begin{cases} rect(\frac{x_0}{2b}) = 1,\ -b \le x_0 \le b \\ rect(\frac{x_0}{2b}) = 0,\ x_0 < -b,\ \text{or} x_0 > b \end{cases}, \tag{14}$$

and

$$\alpha = \sqrt{\frac{KT}{e(u-u_0)}}. \tag{15}$$

Hence, the current density distribution in the paraxial approximation can be derived at any specific cross-section as:

$$j(x) = \frac{j_0 r_0}{2rg}[erf(\frac{x-gb}{h\alpha}) - erf(\frac{x+gb}{h\alpha})], \tag{16}$$

$$erf(z) = \frac{2}{\sqrt{\pi}}\int_0^z \exp(-t^2)dt. \tag{17}$$

After working out current density distributions of all sub-beam units, each current density distribution is converted to the laboratory coordinate system (z, r). The axial direction component j_z is computed and summed to get the total current density distribution for the whole electron beam. The charge density can be calculated as:

$$\rho = \sqrt{\frac{1+r'^2}{-2Q_0(e/m_0)}} j_z. \tag{18}$$

The above curvilinear-axis electron beam model is a practical method for calculating the current density and charge density in electron beams and guns. To calculate the space-charge density, usually the self-consistent space-charge field is calculated by an iterative method. A program is written to solve the electric field corresponding to the space-charge distribution by finite element method. The current density at the cathode is computed using a modified Child's law considering the virtual cathode formed by longitudinal initial thermal

https://doi.org/10.1017/S0263034614000421 Published online by Cambridge University Press

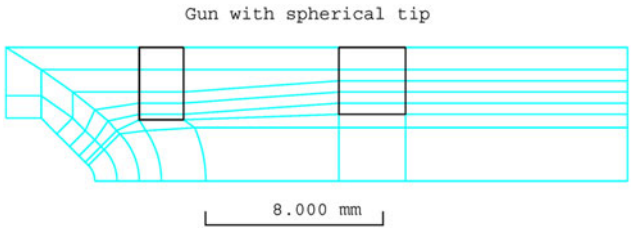

Fig. 1. (Color online) Finite element course mesh layout for a gun with spherical tip.

velocities. The method above is adopted to compute iteratively the current density and space-charge density distributions. This method is simple and the program is very compact.

3. DETERMINING THE VIRTUAL INTERSECTION OF ELECTRON GUNS

As we described in Section I, when the current density of each toroidal sub-beam is calculated, the distance to the axis r_e and the slope r_e' of the central rays, and current density j_e along the z-axis direction of each sub-beam unit at the exit plane of the guns are obtained, the subscript e denotes the exit plane. Hence, the virtual intersection can be derived using the curvilinear-axis theory. In the calculation of the virtual intersection, the potential is assumed to be equivalent at the gun region to simplify the calculation. For the trajectory projected back toward the cathode at the exit plane, two linearly independent special solutions $g(z)$ and $h(z)$ of Eq. (8) can be derived as:

$$g = 1, h = x - x_e. \tag{19}$$

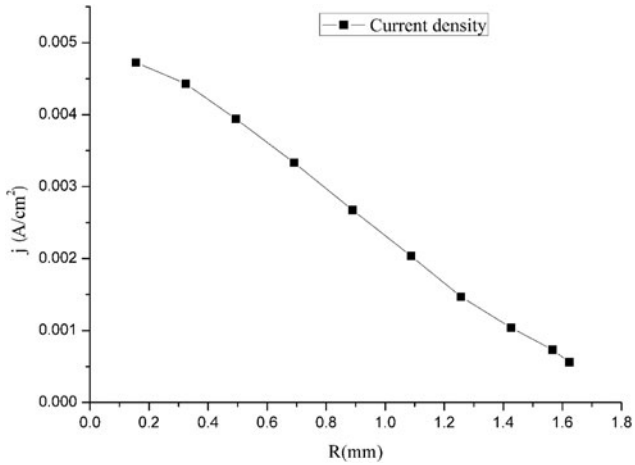

Fig. 3. Current density at the exit plane using the modified software.

Introducing Eq. (19) to Eq. (16), the current density distribution can be derived:

$$j(x) = \frac{j_e r_e}{2r}[erf(\frac{x - b_e}{(x - x_e)\alpha}) - erf(\frac{x + b_e}{(x - x_e)\alpha})]. \tag{20}$$

It must be noticed that the special solution $h(z)$ is always negative at the guns region. If the beam is focused at the exit plane, the potential at the region behind the exit plane can be assumed to be equivalent. Thus, the special solution $h(z)$ is positive. Using the same method, the current density distribution behind the exit plan can be achieved. The position with the maximum of the current density along the z-axis direction is the virtual intersection. Additionally, the radius of the virtual crossover can be achieved.

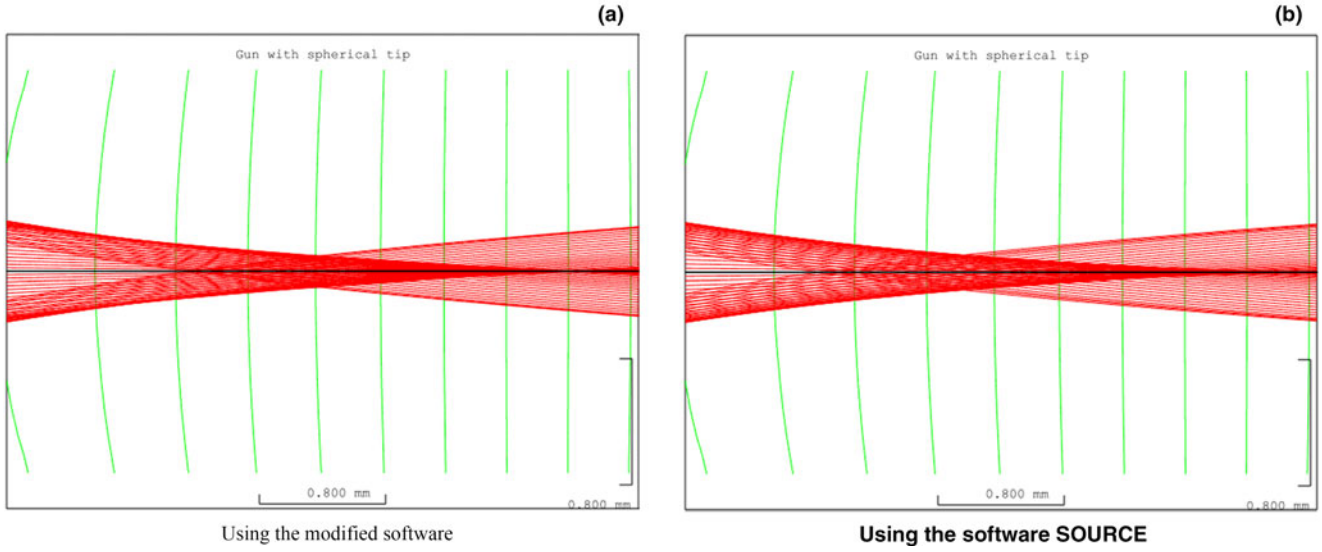

Fig. 2. (Color online) Electron trajectories and equipotentials of an electron gun with spherical tip calculating using two methods (the first equipotential surface at the position of $z = 7.00$ mm).

https://doi.org/10.1017/S0263034614000421 Published online by Cambridge University Press

4. COMPUTATION EXAMPLES

As an example, a practical electron gun is sketched in Figure 1. It is calculated using the modified software and the result is compared with that calculated using SOURCE. The calculations are performed with the same interactive error, the cathode temperature at 1600 K, the work function 2.7eV, and Richardson constant 60 $A/cm^2/deg^2$ for the two methods.

The computed results show that the total emission current is of 1933.02 μA, and the position of virtual crossover is 7.96 mm (at the spherical tip of the cathode, $z = 0.00$ mm) using the modified software. In contrast, using SOURCE the total emission current is 2746.32 μA, the position of virtual crossover is 8.28 mm. Compared with SOURCE, using the modified software, the total current is decreased, and the crossover is moved away from the cathode, however, the virtual crossover moved closer to the cathode. Electron trajectories and equipotentials for the two methods are shown in Figure 2. Figure 3 shows the current density at the exit plane using the modified software. As a second example, a LaB_6 electron gun is simulated. The finite element course mesh layout is shown in Figure 4. We assumed that the emission properties are different in the different regions along the cathode surface. Thus, the cathode was divided into three parts, in all three emission regions, the work function is set at 2.70 eV, the Richardson constant at 70 $A/cm^2/deg^2$, and cathode temperature in the first, second, and third emission are set at 1770 K, 1820 K, and 1870 K, respectively. The computed results using the modified software show that the virtual crossover is 6.91 mm, and

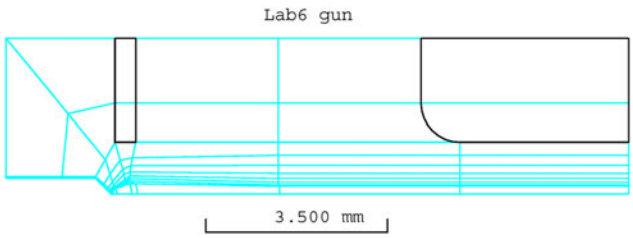

Fig. 4. (Color online) Finite element course mesh layout for a LaB6 gun.

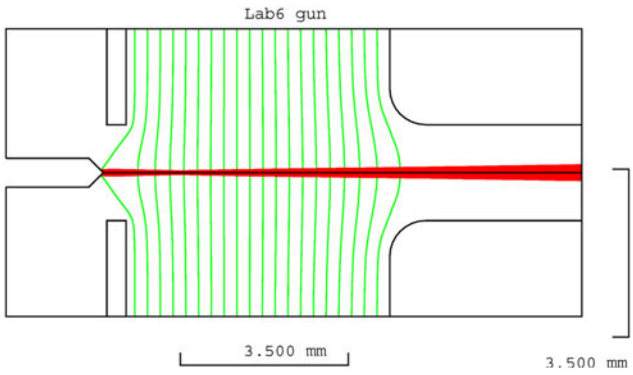

Fig. 5. (Color online) Electron trajectories and equipotentials of a LaB6 gun.

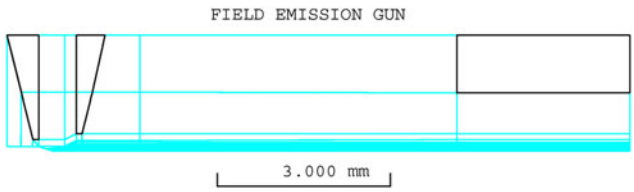

Fig. 6. (Color online) Finite element course mesh layout for a field emission gun.

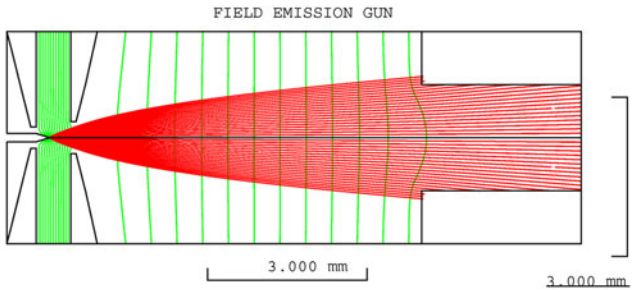

Fig. 7. (Color online) The electron trajectories and equipotentials of a field emission gun.

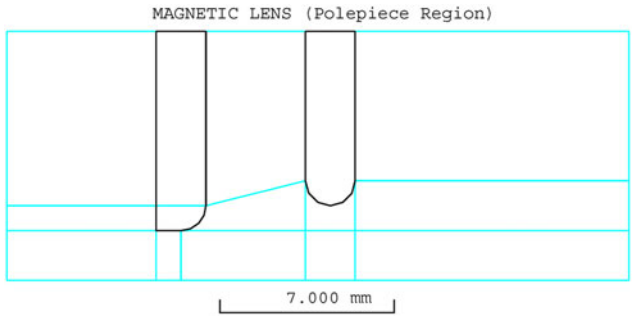

Fig. 8. (Color online) Finite element course mesh layout for a field emission gun with a magnetic lens.

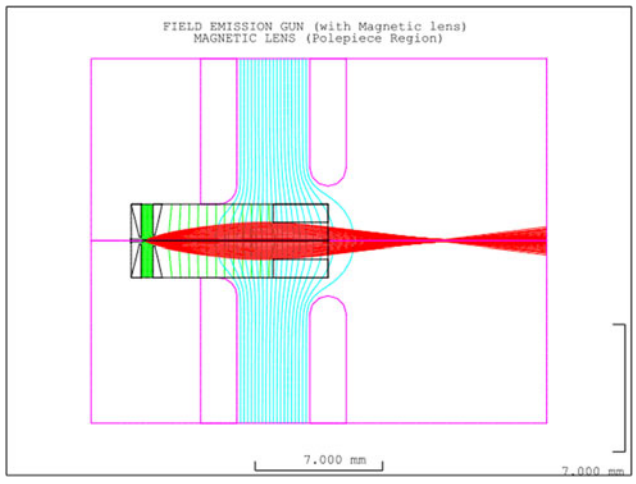

Fig. 9. (Color online) Electron trajectories and equipotentials of a field emission gun with a magnetic lens.

https://doi.org/10.1017/S0263034614000421 Published online by Cambridge University Press

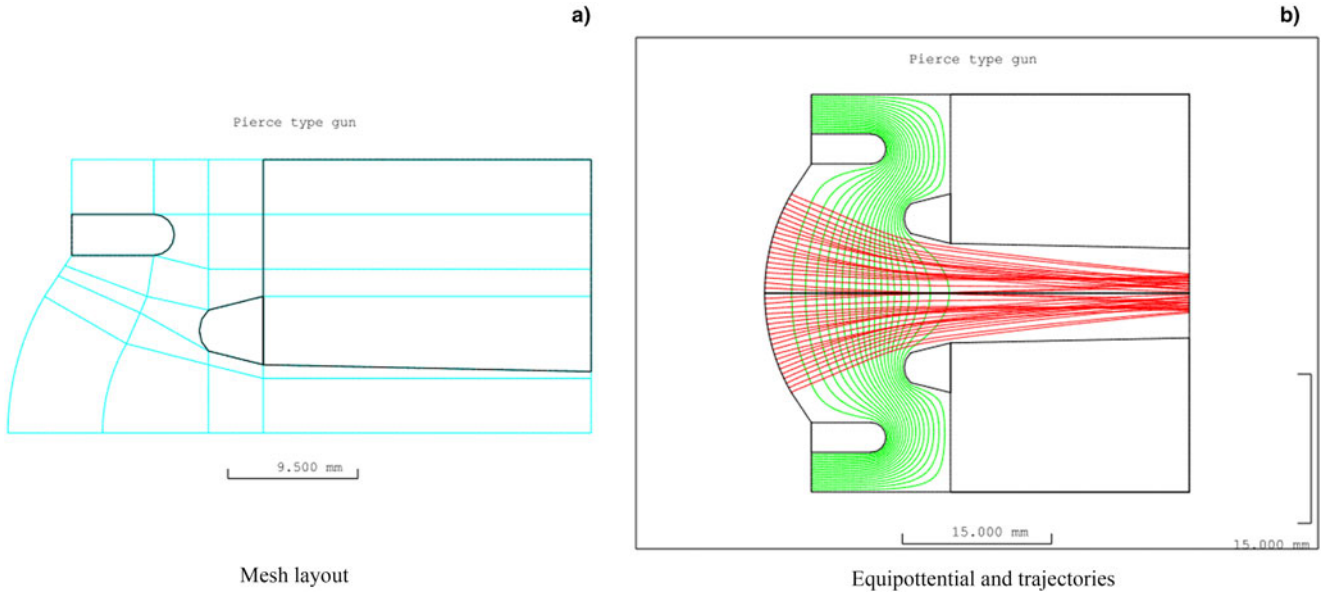

Fig. 10. (Color online) A pierce gun example.

the radius of the virtual crossover is 5.95 μm. The electron trajectories and equipotentials are shown in Figure 5. For the third example, a field emission gun is simulated. The finite element course mesh layout is shown in Figure 6. With a cathode temperature of 300 K, a work function of 4.5eV, and Richardson constant 120 $A/cm^2/deg^2$, the computed results using the modified software show that the virtual crossover is −1.53 mm, and the radius of the virtual crossover is 0.0018 μm. The electron trajectories and equipotentials are shown in the Figure 7.

The equivalent meridional potential is introduced into the modified software. The electric and magnetic fields can be handled in a unified way. To test the modified software for an electron gun with magnetic field, a magnetic lens with a lens excitation of 2000NI (see Fig. 8) is inserted into an emission gun positioned 7 mm away from the cathode. This field emission gun produces a crossover because of magnetic lens. The computed results using the modified software are shown in Figure 9. It shows that the position of the virtual crossover is 17.65 mm with the radius of the virtual crossover is 0.0025 μm

At last, a Pierce gun with high-current is simulated. In this case, the space charge effect is very important in numerical calculation and can be well-treated using the modified software. Figure 10a shows the finite element course mesh layout. Figure 10b shows the computed equipotential and trajectories. The above examples demonstrate that the modified software performs very well. The results show that this approach is a feasible way for calculating high-current guns considering thermal velocity effects.

5. CONCLUSION

The initial thermal velocity and space charge effects of electron beams significantly limit the performance of electron guns. Adequately taking these two factors into account in numerical calculations of current density distribution of electron guns is a very complicated problem. By introducing the curvilinear axial evolution theory of the current and charged density, the current density distribution can be computed in an iteration calculation by adding the current density generated by all the sub-beams. Moreover, the charge density distribution can be calculated, from which the virtual intersection can be derived. Based on these methods, the numerical calculation software SOURCE for electron guns simulations is now greatly improved. The tungsten cathode gun, the LaB_6 cathode gun, the field mission gun and the Pierce gun are simulation using the modified software respectively. The simulation results demonstrate that the modified software is more effective and more practical.

ACKNOWLEDGMENT

This work is sponsored by the National Natural Science Foundation of the People's Republic of China (61001040). We sincerely appreciate this support.

REFERENCES

Burdovitsin, V.A. & Oks, E.M. (2008). Fore-vacuum plasma-cathode electron sources. *Laser Part. Beams* **26**, 619–635.

Culter, C.C. & Hines, M.E. (1955). Thermal velocity effects in electron guns. *Proc. IRE* **43**, 307–315.

Hawkes, P.W. & Kasper, E. (1989). *Principles of Electron Optics*. London: Academic.

Morrell, A.M., Law, H.B., Ramberg, E.G. & Herold, E.W. (1974). *Color Television Picture Tubes*. New York: Academic.

Munro, E. (1997). Computational techniques for design of charged particle optical systems. In *Handbook of charged Particle Optics* (Orloff, J., ed.), pp.1–74. Boca Raton: CRC Press.

https://doi.org/10.1017/S0263034614000421 Published online by Cambridge University Press

Ozur, G.E., Proskurovsky, D.I. & Rotshtein, V.P. *et al.* (2003). Production and application of low-energy, high-current electron beams. *Laser Particle Beams* **21**, 157–174.

Septier, A. (1983). *Applied Charged Particle Optics*. New York: Academic.

Stratton, J.A. (1941). *Electromagnetic Theory*. New York: McGraw-Hill.

Tang, T.T. & Kang, Y.F. (2005). A new approach for evaluating the current and charge density distributions in electron guns and beams. *Optik* **116**, 185–193.

Tang, T.T. (1986). *Introduction to Applied Charged Particles Optics (in Chinese)*. Xi'an: Xi'an Jiaotong University Press.

Tang, T.T. (1996). *Advanced Optical Electronics (in Chinese)*. Beijing: Beijing Science-Technology University Press.

Tang, T.T. (1982). Second and third order aperture aberrations of uniform magnetic field spectrometers. *Optik* **62**, 379–399.

Villa, F. & Luccio, A. (1997). Test of a high-gradient low-emittance electron gun. *Laser Particle Beams* **15**, 427–447.

Weber, C. (1967). Analogue and digital methods for investigating electron-optical systems. *Philips Res. Rep. (Suppl.)* **6**, 1–95.

Zhu, X.Q. & Munro, E. (1989). A computer program for electron gun design using second-order finite elements. *J. Vac. ScI. Technol.* **B 7**, 1862–1869.

https://doi.org/10.1017/S0263034614000421 Published online by Cambridge University Press